

1  
2  
3  
4  
5  
6  
7  
8  
9  
10  
11  
12  
13  
14  
15  
16  
17  
18  
19

**Assessing the accuracy of predicted ocean tide loading displacement values**

**N.T. Penna<sup>1</sup> · M.S. Bos<sup>2</sup> · T.F. Baker<sup>3</sup> · H.-G. Scherneck<sup>4</sup>**

<sup>1</sup>School of Civil Engineering and Geosciences, Newcastle University, Newcastle upon Tyne,  
NE1 7RU, UK

E-mail: nigel.penna@ncl.ac.uk

<sup>2</sup>Astronomical Observatory, University of Porto, Monte da Virgem 4430-146, Vila Nova de  
Gaia, Portugal

<sup>3</sup>Proudman Oceanographic Laboratory, 6 Brownlow Street, Liverpool, L3 5DA, UK

<sup>4</sup>Onsala Space Observatory, Chalmers University of Technology, Sweden

20 **Abstract** The accuracy of ocean tide loading (OTL) displacement values has long been  
21 assumed to be dominated by errors in the ocean tide models used, with errors due to the  
22 convolution scheme used considered very small (2-5%). However, this paper shows that much  
23 larger convolution errors can arise at sites within approximately 150 km of the coastline,  
24 depending on the method used to refine the discrete regularly spaced grid cells of the ocean tide  
25 model to better fit the coastline closest to the site of interest. If the local water mass  
26 redistribution approach is implemented, as used in the OLFG/OLMPP software recommended in  
27 the IERS 2003 conventions, OTL height displacement errors of up to around 20% can arise,  
28 depending on the ocean tide model used. Bilinear interpolation only, as used in the SPOTL and  
29 CARGA softwares for example, is shown from extensive global and regional comparisons of  
30 OTL displacement values derived from the different methods and softwares to be more  
31 appropriate. This is verified using GPS observations. The coastal refinement approach used in  
32 the OLFG/OLMPP software was therefore changed in August 2007 to use bilinear interpolation  
33 only. It is shown that with this change, OTL displacement values computed using  
34 OLFG/OLMPP, SPOTL and CARGA invariably agree to the millimetre level for coastal sites,  
35 and better than 0.2 mm for sites more than about 150 km inland.

36

37 **Keywords** Ocean tide loading (OTL) · Displacement · Ocean tide models

38

## 39 **1 Introduction**

40

41 The periodic distribution of water due to the ocean tides loads the Earth, such that in some areas  
42 such as south-west England the surface moves through a (predominantly) vertical range of over  
43 100 mm in around 6 hours. The measurement of this ocean tide loading (OTL) displacement  
44 with GPS and VLBI has seen much progress in recent years, with studies by Allinson et al.  
45 (2004), King et al. (2005), Thomas et al. (2007) and Petrov and Ma (2003) demonstrating an  
46 attainable measurement quality of around 1 mm at discrete sites where many years of  
47 GPS/VLBI data are available. Ideally the OTL displacement should also be predicted  
48 (modelled) to this accuracy or better, in order to remove the phenomenon adequately from  
49 geodetic measurements so as not to bias the resulting coordinate and baseline time series.

50

51 OTL displacements can be modelled by convolving a global ocean tide model with a Green's  
52 function that depends on the elasticity of the Earth. Errors in the different available ocean tide  
53 models have long been considered to dominate the errors in the OTL values (Scherneck 1993;  
54 Bos and Baker 2005). The numerical errors in the convolution scheme have been studied by  
55 Agnew (1997) by comparing the output of different OTL programs with the same input. He  
56 found that the differences (at an unspecified number and distribution of sites) were usually less  
57 than 5% and often less than 2%. Bos and Baker (2005) undertook a similar investigation with  
58 newer loading programs that included SPOTL v3.1 (Agnew 1997), GOTIC2 (Matsumoto et al.  
59 2001), OLFG/OLMPP (Scherneck 1991) and CONMODB (the program used at the Proudman  
60 Oceanographic Laboratory), and selected from each program the best methods to construct a  
61 new program called CARGA. On considering 10 globally distributed superconducting  
62 gravimeter sites all at least, but invariably much more than  
63 50 km inland, they demonstrated a 2-5% (better than 1% for inland European sites) numerical

64 error for the OTL convolution procedure. Although the accuracy of the ocean tide models has  
65 improved dramatically during the 1990s (Shum et al. 1997), they are still considered to cause  
66 most of the uncertainty in OTL values.

67

68 Modern global ocean tide models are provided on evenly distributed grids ( $0.125^\circ$ ,  $0.25^\circ$  or  $0.5^\circ$   
69 spacing typically) and therefore the grid cells do not fit the coastline perfectly. This results in a  
70 misrepresentation of the tidal water mass that is causing the OTL. To improve the accuracy of  
71 the OTL computation it is therefore necessary to refine the ocean tide model grid locally, i.e. by  
72 interpolating the model to a finer grid. The tidal values in the refined grid are mostly  
73 determined with bilinear interpolation. Scherneck (1991) describes a further requirement  
74 whereby local water mass redistribution (MRD) is undertaken in order that the water mass  
75 within the area of refinement remains constant. This MRD approach was used in the 'OTL web  
76 provider' (<http://www.oso.chalmers.se/~loading/>) from its inception in 2001 until August 2007,  
77 when it switched to using bilinear interpolation only, as a result of the findings described in this  
78 paper. The methods used in the OTL web provider are important since it facilitated the wide  
79 and easy access to modelling OTL displacement by the space geodetic community, and is the  
80 approach recommended in the IERS 2003 conventions (McCarthy and Petit 2004). Therefore  
81 many GPS, DORIS, SLR and VLBI-based research projects have used such values, including  
82 both global (Urschl et al. 2005; Thomas et al. 2007) and local (Melachroinos et al. 2007)  
83 comparisons of predicted OTL displacement values with GPS observations. What has never  
84 been tested however, is whether MRD should be carried out when using modern global ocean  
85 tide models or if bilinear interpolation alone is sufficient, and what the influence of this choice is  
86 for both coastal and inland sites when millimetre or better accuracy is desired. This is  
87 investigated in this paper. Also detailed are global and regional comparisons of OTL  
88 displacements computed from different software packages that use different refinement methods

89 for ocean tide model grid cells that overlap land. The sensitivity of the choice of model  
90 refinement method to the particular ocean tide model input is illustrated, and an indication  
91 provided of the quality of the different ocean tide models, for both coastal and inland sites.

92

## 93 2 Ocean tide loading computation and softwares

94

### 95 2.1 Ocean tide loading computation

96

97 For each tidal frequency (the M2 constituent with period 12.42 h usually dominates) the OTL

98 displacement  $u$  at the discrete site at  $r$  can be computed with the following convolution

99 integral (Longman 1962, 1963):

100

$$101 \quad u(r) = \int_{\Omega} \rho G(|r - r'|) Z(r') d\Omega \quad (1)$$

102

103 In Eq. (1),  $\rho$  represents the density of sea water and  $Z$  is the tide at  $r'$ , whilst  $G$  is a Green's

104 function that depends only on the distance between  $r$  and  $r'$ . The integral is taken globally

105 over all water areas  $\Omega$ , thus requiring the use of a global ocean tide model.

106

107 A focus of this paper is the influence of the near ocean tides on the computed OTL values. To

108 illustrate the effect of the tides near the site of interest, consider an example in which the

109 coastline is straight, the site is exactly on this coastline and that only the loading due to the tides

110 within a radius of  $r$  around the site (which thus forms a half circle) is taken into account. Using

111 the equation for a point load on an homogeneous half-space (Farrell 1972), the amplitude of the

112 OTL height displacement  $u$  at the site is given by:

113

$$114 \quad u = \frac{3\rho}{4\rho_E a} h_{\infty} Z r \approx -1.1 \times 10^{-7} Z r \quad (m) \quad \text{for } r < 10 \text{ km} \quad (2)$$

115

116 where  $\rho_E$  is the mean density of the solid Earth,  $a$  is the mean radius of the Earth (assumed  
117 spherical),  $Z$  is the amplitude of the ocean tide and  $h_\infty$  is the Love number for a homogeneous  
118 half-space (Farrell 1972). The units of  $Z$  and  $r$  are m. Similarly, the horizontal displacement  
119  $v$ , perpendicular to the straight coastline, due to a half circle, is given by:

120

$$121 \quad v = \frac{3\rho}{2\pi\rho_E a} l_\infty Z r \approx 0.24 \times 10^{-7} Z r \text{ (m) for } r < 10 \text{ km} \quad (3)$$

122 where  $l_\infty = 1.673$ . Thus the height displacement is about 4.7 times larger than the horizontal  
123 displacement.

124

125 Eq. 2 illustrates that the contribution of a 1 m tide to the OTL height displacement within a 10  
126 km radius of the site is around 1 mm, showing that the near tides can have a significant  
127 contribution to the loading value. For a larger radius of 100 km one should take roughly half the  
128 value of  $h_\infty$ , to take into account the fact that the Earth is not homogeneous but consists of  
129 different elastic layers, which results in a 5 mm displacement for a 1 m tide. Consequently,  
130 within this radius the amplitude of the tides must be known to better than  
131 20 cm to reach a 1 mm accuracy threshold. These examples demonstrate that both near and far  
132 tides must be considered when computing OTL values, with the near tides being the most  
133 important.

134

135

## 136 2.2 OTL softwares

137

138 The different OTL software packages all compute Eq. (1). Since near tides have the biggest  
139 contribution to the loading at a site yet the global ocean tide models are only provided as  
140 discrete values on regularly spaced grids, an important feature of each package is how the grid is  
141 refined and interpolated to a finer resolution in the cells nearest the site considered, to better fit  
142 the coastline. A finer grid near the site of interest also helps assure that the approximation of the  
143 continuous loading by point masses best represents reality. The effect of coastal grid refinement  
144 on OTL values decreases for more inland sites.

145

146 Three different software packages are considered in this paper (OLFG/OLMPP, SPOTL and  
147 CARGA), chosen since they are widely used and freely distributed or use different approaches  
148 to ocean tide model refinement at the coast. Key features of each package are now précised,  
149 particularly regarding their methods of coastal model refinement. Further details on each  
150 package are provided in Bos and Baker (2005).

151

152 OLFG/OLMPP was selected since it is used by the popular OTL web provider recommended in  
153 the IERS 2003 conventions. The area of coastal model refinement comprises a  $3^{\circ}\times 3^{\circ}$  box  
154 around the site considered, and within this box interpolation and extrapolation is performed by  
155 considering all tides within a  $5^{\circ}\times 5^{\circ}$  box surrounding the site. The box boundaries are not  
156 defined from exact centering about the site however, but instead are chosen to fit the nearest grid  
157 lines of the ocean tide model. A further (unique) feature is the use of MRD across the  $3^{\circ}\times 3^{\circ}$   
158 box, i.e. to avoid creating or destroying water within the box, the excess tidal water mass is  
159 redistributed equally over all water surfaces. Thus, if the water area is larger after refinement of  
160 the grid, then the tidal amplitude will locally be reduced and vice versa. Outside the  $3^{\circ}\times 3^{\circ}$  box

161 the model is not refined, meaning that for sites far enough (more than ~150 km) inland, no  
162 attempt is made to compensate for model cells imperfectly fitting the coastline. The value for  
163 the density of sea water used is  $1030 \text{ kg/m}^3$ .

164

165 SPOTL is a freely distributed package that uses concentric rings around the site considered to  
166 represent the integration mesh. The width of the rings and number of subdivisions is dependent  
167 on the distance from the site, but within a  $10^\circ$  radius bilinear interpolation is used to refine the  
168 mesh to better fit the coastline, whilst outside the tide value for a given location simply takes the  
169 value of the model grid cell that covers that location. This means that for sites far enough inland  
170 (defined as a  $10^\circ$  radius, i.e. approximately 1000 km), no model coastal refinement takes place.  
171 The value for the density of sea water used is  $1025 \text{ kg/m}^3$ .

172

173 CARGA uses bilinear interpolation to refine the model for every cell across the globe that  
174 imperfectly fits the coastline, rather than only refining the model locally. Bilinear interpolation  
175 is also used to compute the tide in the open ocean, rather than the SPOTL approach of using the  
176 value of the nearest grid cell. The OTL displacement value output from CARGA is a mean of  
177 18 runs, in which three mesh layouts, two different coastlines and three coastal interpolation  
178 techniques are varied. The value for the density of sea water is kept fixed to  $1030 \text{ kg/m}^3$ .  
179 Global tidal water mass is conserved (to ensure that no water mass is created or destroyed  
180 during the tidal cycle) by removing a small uniform layer, whose thickness is different for each  
181 ocean tide model and constituent considered (Bos and Baker 2005).

182

183 This section has considered OTL displacement. The effects of gravity OTL at (near) coastal  
184 sites are more complicated since the direct gravitational attraction of the tidal water mass  
185 dominates the OTL value. A very high resolution coastline is necessary together with a very

186 accurate value of the ocean tides in front of the site (Bos et al. 2002). The gravity OTL  
187 computation cannot yet be accurately automated for (near) coastal sites and therefore is not  
188 considered in this paper.

189

### 190 **3 Ocean tide models**

191

192 The global ocean tide models ('maps') input to OTL softwares are mostly computed with the  
193 use of the Laplace tidal equations which are depth integrated (Hendershott and Munk 1970).  
194 For each tidal constituent, a global map of tidal amplitudes and phase-lags relative to the tidal  
195 gravitational potential at the Greenwich meridian is obtained. These hydrodynamic solutions do  
196 not represent the true tides perfectly and for that reason the solutions are adjusted to fit tidal  
197 observations. The Schwiderski (1980) tide model was one of the first successful examples of  
198 using tide gauge data to improve the model. The most recent models assimilate tide gauge and  
199 (usually TOPEX/POSEIDON) satellite altimetry data to improve the accuracy of their tide  
200 model, and a short description of the most used ones is given below. Each of the models  
201 described is distributed to the community as a set of amplitude and phase values on discrete,  
202 regularly spaced global grids.

203

204 NAO.99b (Matsumoto et al. 2000) is based on the same hydrodynamics as the Schwiderski  
205 model but includes the assimilation of TOPEX/POSEIDON data. It is provided (and directly  
206 computed) on a  $0.5^\circ$  grid and hence the misfit with the coast can be as large as 25 km. The Ross  
207 Sea is not modelled.

208

209 FES94.1 (Le Provost et al. 1994) is a pure hydrodynamic tide model tuned to fit tide gauges  
210 globally. It has been calculated on a finite element grid with very fine resolution near the coast  
211 but has been transformed on to a regular  $0.5^\circ$  grid for its distribution. It is no longer used  
212 because it has been superseded by FES99 (Lefèvre et al. 2002) which includes the assimilation  
213 of tide gauge and TOPEX/POSEIDON data. FES99 is transformed to a  $0.25^\circ$  grid for  
214 distribution, and although its resolution is better than FES94.1, it has too many grid cells over

215 land. FES99 does not have any tidal information in the Baltic Sea, the Black Sea, the Persian  
216 Gulf or the Red Sea. The most recent FES version is FES2004 (Lyard et al. 2006) which has a  
217 very good fit to the coastline (although the ice shelf in the Ross Sea is modelled ~100 km inland  
218 of the grounding zone) and is provided on a 0.125° grid.

219  
220 GOT00.2 (Ray 1999) was developed by adjusting the hydrodynamic model FES94.1 using  
221 TOPEX/POSEIDON and ERS 1/2 satellite altimetry observations. It is provided on a 0.5° grid  
222 and incorporates local models of the tides in the Gulf of Maine, the Gulf of St Lawrence, the  
223 Persian Gulf, the Mediterranean Sea and the Red Sea.

224  
225 TPXO.6.2 (Egbert and Erofeeva 2002) is a model into which tide gauge (from the Arctic Ocean  
226 and around Antarctica) and TOPEX/POSEIDON data have been assimilated using the procedure  
227 described by Egbert et al. (1994). It is provided (and directly computed) on a 0.25° grid and  
228 does not contain the Black Sea.

229  
230 A further model is CSR3.0 (Eanes and Bettadpur 1996) which applies long wavelength  
231 corrections to FES94.1 via 2.4 years of TOPEX/POSEIDON data, whilst CSR4.0 is an update  
232 using a longer data span. It is provided on a 0.5° grid. Outside the ±66° TOPEX/POSEIDON  
233 coverage limits, the model defaults to FES94.1.

234

235

236

#### 237 **4 Global comparison of OTL softwares**

238

239 To investigate the effects of the ocean tide model coastal refinement method used and the  
240 sensitivity of both coastal and inland sites to it, all 387 sites (as of August 2007) of the IGS  
241 (Dow et al. 2005) network were selected. This provided a global distribution of sites often  
242 analysed by the space geodetic community. M2 OTL height, east and north displacements were  
243 computed using the OLFG/OLMPP (applying MRD), SPOTL v3.2 and CARGA softwares. For  
244 each software, the computed OTL values represent displacements of the Earth's surface relative  
245 to the centre of mass of the undeformed solid Earth without atmosphere and oceans (this  
246 convention was used throughout this paper). Firstly the FES99 model was input since it is one  
247 of two (the other being GOT00.2) recommended in the IERS 2003 conventions for the  
248 computation of OTL. Then the more recent FES2004 model was input, that has a very good fit  
249 to the coastline and a finer grid resolution of  $0.125^\circ$  than the  $0.25^\circ$  resolution FES99 model. The  
250 agreements between the OTL displacements computed per software for each model were  
251 assessed by computing, per component per site, the vector difference:

252

$$253 \quad d = \sqrt{(A_1 \cos \varphi_1 - A_2 \cos \varphi_2)^2 + (A_1 \sin \varphi_1 - A_2 \sin \varphi_2)^2} \quad (4)$$

254

255 where  $d$  is the vector difference and  $A_i$ ,  $\varphi_i$  respectively represent, per software, the OTL  
256 displacement amplitude and Greenwich phase lag.

257

258 For the height component, vector differences were computed between the OLFG/OLMPP  
259 (MRD) and CARGA values, and between the SPOTL and CARGA values, which are plotted in  
260 Fig. 1. It is immediately apparent that the SPOTL and CARGA values invariably agree at the  
261 sub-mm level for both the FES99 and FES2004 models. In fact, as can be seen from Table 1,

262 the agreement between CARGA and SPOTL is better than 0.2 mm at 298 sites when using  
263 FES99, and at 318 sites when using FES2004. At only five and six sites is the agreement worse  
264 than 1 mm for FES99 and FES2004 respectively. For FES99 the maximum difference is 2.43  
265 mm at VESL (lon. 357.1583, lat. -71.6738) in Antarctica, followed by 1.53 and 1.36 mm at  
266 NANO (lon. 235.9135, lat. 49.2948) and ALBH (lon. 236.5126, lat. 48.3898) respectively,  
267 which are both on Vancouver Island. For FES2004 the maximum difference of 2.23 mm also  
268 occurs at VESL, followed by 1.57 mm at EPRT (lon. 293.0079, lat. 44.9087) on the Bay of  
269 Fundy. The difference at VESL is due to a newer coastline in SPOTL (v3.2) than CARGA  
270 (which uses the SPOTL v3.1 coastline), whilst around Vancouver Island the large FES99  
271 differences are likely to be caused by a large gap between the model grid and land, resulting in  
272 much extrapolation by CARGA.

273  
274 The differences shown in Fig. 1 between the OLFG/OLMPP (MRD) and CARGA height values  
275 are strikingly much greater for the FES99 model than the equivalent SPOTL minus CARGA  
276 differences. Table 1 details that 34 of these differences are greater than 1 mm, which all arise at  
277 coastal sites. Meanwhile, only 199 (compared with 298 for SPOTL-CARGA) of the differences  
278 are less than 0.2 mm. However, when using FES2004, at only four sites are the differences  
279 greater than 1 mm, and at 350 sites the differences are less than 0.2 mm. This clearly suggests  
280 that the model refinement method employed by OLFG/OLMPP (MRD) is not equivalent to  
281 those of SPOTL and CARGA for coastal grid cells when using the FES99 model, although all  
282 three methods work equivalently for the FES2004 model. The striking FES99 OLFG/OLMPP  
283 (MRD) discrepancies arise since many of the FES99 grid cells overlap the land (due to an  
284 inaccurate transformation from the irregular grid in the computed version to the regular global  
285 grid in the distributed version), and the MRD approach requires this excess to be redistributed  
286 evenly across the  $3^{\circ} \times 3^{\circ}$  refinement box. This can change the model's tidal amplitude for cells

287 within about 150 km of the site by up to about 20% and hence the near tide loading effect  
288 changes. The FES99 model tendency for the grid cells to overlap the land is not exhibited in  
289 FES2004. Thus little excess water mass arises and applying MRD has little effect on the  
290 loading values compared with those computed using bilinear interpolation of the model's grid  
291 cells alone. In addition, the finer 0.125° grid of FES2004 also diminishes the difference of using  
292 the nearest grid cell (SPOTL) instead of bilinear interpolation (CARGA and OLFG/OLMPP) to  
293 determine the tidal amplitude in the open ocean.

294  
295 To confirm that the large discrepancies between OLFG/OLMPP (MRD) and CARGA (and  
296 implicitly also SPOTL) height values when inputting the FES99 model arise from employing  
297 MRD, the OLFG/OLMPP values were recomputed but without employing MRD when refining  
298 the land overlapping model cells in the 3°×3° box around the site. **Thus only bilinear**  
299 **interpolation was carried out.** These solutions are referred to as OLFG/OLMPP (NoMRD). The  
300 OLFG/OLMPP (NoMRD) minus CARGA differences when using both the FES99 and  
301 FES2004 models are also shown in Fig. 1. The discrepancies between the OLFG/OLMPP and  
302 CARGA FES99 values are clearly now much smaller and, as detailed in Table 1, 286 sites have  
303 differences less than 0.2 mm, and only five sites have differences greater than 1 mm. As with  
304 the SPOTL minus CARGA comparisons, the biggest differences arise at NANO (due to much  
305 CARGA extrapolation) and VESL. The VESL differences arise since OLFG/OLMPP uses the  
306 GMT (Wessel and Smith, 1998) coastline which, in Antarctica, follows the ice shelves instead  
307 of the land-sea interface followed by the CARGA (SPOTL v3.1) coastline. For the FES2004  
308 model, the OLFG/OLMPP (NoMRD) values are practically identical to the OLFG/OLMPP  
309 (MRD) values, as can be gleaned by comparing the similarity in the CARGA comparison  
310 statistics listed in Table 1. In the FES2004 distribution the grid fits the coast much better,  
311 without the tendency to always overlap the coast.

312

313 The equivalent horizontal displacement vector differences are shown in Tables 2 and 3 for the  
314 east and north components respectively. It is clearly apparent that the four approaches are in  
315 much closer agreement (as judged by the absolute values of the vector differences) for the  
316 horizontal components than the height, and the effect of MRD is less pronounced. For both the  
317 FES99 and FES2004 models, none of the OLFG/OLMPP (MRD) minus CARGA, SPOTL  
318 minus CARGA or OLFG/OLMPP (NoMRD) minus CARGA differences exceed 1 mm, all but  
319 3-4 are less than 0.5 mm, and for at least 90% of sites the differences are less than 0.2 mm  
320 (invariably substantially so). For the north component, the biggest differences arise for the  
321 Antarctic sites OHI2 (lon. 302.0987, lat. -63.3211), RIO2 (lon. 292.2489, -lat. 53.7855) and  
322 VESL, which is attributed to the different OLFG/OLMPP and CARGA coastlines. Meanwhile,  
323 the largest differences (0.7 mm) between the OLFG/OLMPP (MRD) and CARGA east  
324 component values arise for the southern England sites HERS (lon. 0.3362, lat. 50.8673), HERT  
325 (lon. 0.3344, lat. 50.8675) and NPLD (lon. 359.6604, lat. 51.4210) with the FES99 model. This  
326 is attributed to firstly, the fact that the east component OTL values are large at these locations  
327 (around 6 mm); secondly, the MRD effect causes a difference of 0.2-0.3 mm; and thirdly, the  
328 3°x3° box is too small to remove all FES99 grid cells overlapping the land in the region which at  
329 these locations have large tidal amplitudes. The last effect is around 0.3-0.4 mm. Invariably the  
330 effect of MRD on the horizontal displacements is smaller than for the height in a relative sense  
331 also. In almost all cases, only tiny changes of <5% arise, usually much less so.

332

333 The global discrete IGS site comparisons have shown that OTL displacements are sensitive to  
334 the grid cell refinement method adopted to make the ocean tide model better fit the coastline,  
335 which in turn is model dependent. The largest differences between the CARGA and the  
336 respective OLFG/OLMPP (MRD), OLFG/OLMPP (NoMRD) and SPOTL values all arose at

337 coastal sites. This is to be expected since the near tides have the biggest contribution to the  
338 loading at a site, and no model fits the coastline perfectly. However, only a few of the discrete  
339 sites of the IGS network are located on complicated coastlines and therefore do not necessarily  
340 provide an indication of the biggest discrepancies that can arise, or the spatial scales over which  
341 the discrepancies can change. This is considered in the next section, which focuses on the  
342 height component, since it exhibits much bigger differences than the horizontal components.

343

344

## 345 **5 Regional comparison of OTL softwares**

346

347 To further test the methods of coastal ocean tide model refinement, M2 OTL height  
348 displacements were computed per point of a  $0.125^\circ$  grid across north-west Europe, extending  
349 from  $10^\circ\text{W}$  to  $10^\circ\text{E}$  and  $45^\circ\text{N}$  to  $60^\circ\text{N}$ . The region was selected since it encompasses  
350 complicated coastlines (which the model grid cells do not perfectly fit) around Great Britain and  
351 Brittany, which are surrounded by shallow seas where the modelling of ocean tides is  
352 challenging. The region extends several hundred kilometres inland to substantial portions of  
353 eastern France, Germany and Switzerland, enabling the effect of coastal model refinement  
354 methods on inland sites to be determined also. Furthermore, the region encompasses a very  
355 wide range of M2 OTL height displacement values, from over 5 cm off south-west England to  
356 near zero in Norway. This is illustrated in the M2 OTL height displacement map shown in Fig.  
357 2, computed for the FES2004 model using the CARGA software. As for the IGS site  
358 comparisons, vector differences were formed, namely OLFG/OLMPP (MRD) minus CARGA,  
359 SPOTL minus CARGA and OLFG/OLMPP (NoMRD) minus CARGA, which are shown in  
360 Figs. 3, 4 and 5 respectively. In addition to the FES99 and FES2004 models used for the IGS  
361 sites, displacements were also computed for the GOT00.2 and NAO.99b models. These were  
362 chosen since they are both distributed on a  $0.5^\circ$  grid, i.e. a coarser spacing than FES99, and  
363 GOT00.2 is also recommended in the IERS 2003 conventions.

364

365 It is clear from Fig. 3 that the vector differences between the displacements computed by  
366 OLFG/OLMPP (MRD) and CARGA are substantial around Great Britain when the FES99,  
367 GOT00.2 and NAO.99b models are input. FES99 results in the biggest differences, greater than  
368 5 mm across all of south-west England and across much of Wales, reaching about 8 mm in and  
369 around the Bristol Channel. Expressed as a proportion of the displacement amplitude, these

370 differences are approximately 10-20%, much greater than the <5% differences previously  
371 reported by Agnew (1997) and Bos and Baker (2005). These differences are even larger than  
372 occurred at the global IGS sites, which is attributed to many of the FES99 model grid cells  
373 overlapping the complicated Great Britain coastline which causes a large MRD effect. With the  
374 exception of East Anglia and parts of Scotland around the Caledonian Canal, the vector  
375 differences everywhere in Great Britain are about 1-3 mm, even 100 km and more inland.  
376 Similarly, at least 1-3 mm vector differences arise throughout Brittany and parts of Normandy,  
377 peaking at about 7 mm. The differences arising using NAO.99b are almost as large as with  
378 FES99, reaching 7-8 mm in northern Brittany (about 20%) although somewhat smaller in south-  
379 west England and Wales (2-3 mm), but reach around 4 mm in western Scotland. The  
380 differences are greater than 1 mm throughout all of inland Brittany, Normandy, the Netherlands  
381 and southern England. Whilst the vector differences arising using the GOT00.2 model are not  
382 as large as when using FES99 or NAO.99b, they are still greater than 1 mm throughout Brittany,  
383 Normandy and Scotland. Maximum differences reach around 4 mm near to Glasgow and on the  
384 Normandy coast. There is a pronounced gridded pattern to the differences, which is attributed to  
385 the OLFG/OLMPP 3°×3° refinement box incrementing in steps equal to the grid spacing of the  
386 tide model, rather than being exactly centred around the site. Thus since the resolution of the  
387 GOT00.2 and NAO.99b models is 0.5° and the displacement differences have been computed at  
388 a 0.125° resolution, a gridded pattern results. It is notable that, despite the coarser grid of  
389 GOT00.2 compared with FES99, the OLFG/OLMPP (MRD) minus CARGA differences are not  
390 as pronounced. This shows that the model's grid resolution itself is not the sole contributor to  
391 how much MRD must take place, but more important is how many grid cells, on average,  
392 overlap the land. As GOT00.2 and NAO.99b have the same 0.5° grid resolution, the smaller  
393 differences arising with GOT00.2 suggest that on average, it has fewer grid cells overlapping the  
394 land. As for the IGS sites, the differences obtained when using FES2004 are very small across

395 all of north-west Europe, peaking at only about 1 mm around the Channel Islands. This  
396 suggests that FES2004 has, on average, a very good fit to the coastline. With the exception of  
397 the FES2004 model, the differences generally only reduce to the sub-0.5 mm level seen for the  
398 majority of IGS sites when further than ~150 km inland.

399

400 From Fig. 4, it can be seen that the vector differences between the SPOTL and CARGA  
401 estimates are much smaller than the OLFG/OLMPP (MRD) minus CARGA differences, for  
402 each of the four models considered. The differences between the SPOTL and CARGA values  
403 are invariably less than 0.5 mm for all four models for all but sites right on the coastline, at  
404 which the differences are usually no more than about 1 mm. These larger coastline differences  
405 are attributed to CARGA taking the average of three extrapolation schemes near the coast,  
406 whilst SPOTL uses only one; the differences are smaller over the open ocean since CARGA and  
407 SPOTL both use simple bilinear interpolation of the four surrounding tidal values. Besides sites  
408 right on the coastline, differences greater than 0.5 mm only arise for the NAO.99b model in a  
409 small (few tens of km) section of the Bristol Channel, reaching up to about 6 mm. This is again  
410 attributed to having too many grid cells overlapping the land. The CARGA values are slightly  
411 larger than those of SPOTL over water because the integral over the water only starts at  $0.02^\circ$   
412 from the site considered in SPOTL, while in CARGA this gap does not exist.

413

414 As found above for the IGS sites, it can be seen from inspection of Figs. 3 and 5 that the  
415 agreement between the OLFG/OLMPP and CARGA displacements dramatically improves for  
416 the NoMRD values than when applying MRD. The differences are approximately sub-  
417 millimetre for all four models everywhere except around the Channel Islands for the FES99,  
418 GOT00.2 and NAO.99b models, parts of southern England for FES99, and parts of north-west  
419 England for NAO.99b. For FES2004 the differences are less than 0.5 mm everywhere except

420 around the Ijsselmeer. Thus in general, the very close agreements between the OLFG/OLMPP  
421 NoMRD and CARGA values (and hence also SPOTL values) suggest that for millimetre level  
422 displacement quality, model refinement of local land overlapping cells only is adequate, rather  
423 than refining all land-overlapping cells globally as is done in CARGA. This is the case for all  
424 the models, whether provided on a 0.5°, 0.25° or 0.125° resolution grid. It should be noted  
425 however that this is only the case for millimetre level displacement, with Bos and Baker (2005)  
426 finding the more global refinement used by CARGA is necessary for high quality gravity sites.

427  
428 It can be seen from Figs 3, 4 and 5 that the agreement between the OLFG/OLMPP (MRD),  
429 OLFG/OLMPP (NoMRD), SPOTL and CARGA displacement values improves on moving  
430 further inland. This is expected since the near tides have the biggest influence on a site's  
431 loading value, and therefore the effect of errors due to model cells not perfectly fitting the  
432 coastline, and inadequate model refinement, reduces. All four solutions agree at the sub-0.2 mm  
433 level for each of the four models input when greater than about 100-200 km from the coast.  
434 Indeed, at distances greater than approximately 150 km inland the OLFG/OLMPP MRD and  
435 NoMRD solutions are identical and use the global ocean tide models in their distributed form,  
436 since no model refinement is carried out as the 3°×3° degree box surrounding the site  
437 encompasses no water. Such inland sites provide a pure indication of the numerical differences  
438 between each of the three softwares.

439

## 440 **6 GPS testing of OTL softwares**

441

442 The OLFG/OLMPP (MRD) M2 OTL height displacements have been shown to be highly  
443 discrepant (up to about 8 mm) compared with the OLFG/OLMPP (NoMRD), SPOTL and  
444 CARGA values when either of the FES99, GOT00.2 or NAO.99b models are used. To test  
445 whether the OLFG/OLMPP (MRD) discrepant values are erroneous, a GPS verification was  
446 carried out. A GPS site was selected as close as possible to the part of north-west Europe where  
447 the maximum OLFG/OLMPP (MRD) minus CARGA disagreement arose for each model.  
448 Hence as illustrated in Fig. 3, GLAS was selected for GOT00.2, MALG for NAO.99b and  
449 APPL for FES99. NEWC was arbitrarily selected to verify the FES2004 displacements, even  
450 though no large discrepancies arose. All available data between 2005.00-2007.00 were obtained  
451 for the four sites from the NERC BIGF (<http://www.bigf.ac.uk>) GPS facility. Location details  
452 for these sites are listed in Table 4, together with OTL displacement values computed using each  
453 different software package.

454

455 The GPS data were processed using GIPSY/OASIS v4 software in a kinematic precise point  
456 positioning strategy outlined by King (2006) and refined by King et al. (2008). This involved  
457 processing in 30 h batches with site coordinates, zenith wet delays and receiver clocks estimated  
458 every 5 minutes, whilst holding fixed final JPL fiducial orbits and Earth rotation parameters.  
459 Ambiguities were not fixed to integers and a  $7^\circ$  elevation cut-off angle was adopted. The 30 h  
460 batches were centred on the UT day (3 h overlap either side), with the site coordinates whose  
461 time-tags matched the central UT day extracted to form continuous time series and to minimise  
462 day-to-day edge effects. OTL displacements were firstly modelled using OLFG/OLMPP  
463 (MRD) values, and the processing then repeated applying the CARGA values. The estimated  
464 site coordinates per solution were thinned to a spacing of 30 min, and linear trends and outliers

465 (defined as greater than 5 times the inter-quartile range) removed. Amplitude spectra of the  
466 height time series were then computed according to the Press et al. (1992) implementation of  
467 Scargle (1982), which are shown in Fig. 6.

468

469 The GPS height time series amplitude spectra shown in Fig. 6 clearly indicate that modelling  
470 M2 OTL displacements computed using CARGA reduces 12.42 h (M2) periodicities to the  
471 height time series noise level, whereas substantial energy remains when OLFG/OLMPP (MRD)  
472 is used. This is obvious for the APPL, GLAS and MALG sites, located in areas where there are  
473 large differences between the OLFG/OLMPP (MRD) and CARGA displacements for the  
474 respective FES99, GOT00.2 and NAO.99b ocean tide models. Given that the OLFG/OLMPP  
475 (NoMRD) displacements are in such close agreement with the CARGA values at these sites, it  
476 strongly suggests that MRD is inappropriate when the FES99, GOT00.2 and NAO.99b models  
477 are used. However, when the FES2004 model that better fits the coastline is used, it can be seen  
478 from Fig. 6 that modelling M2 OTL displacement using OLFG/OLMPP (MRD) or CARGA  
479 reduces the energy at the 12.42 h M2 period to the noise level. This suggests that when using  
480 the FES2004 model, MRD may be implemented in the OLFG/OLMPP solutions without loss of  
481 accuracy because the MRD effect is small.

482

## 483 **7 OTL displacement sensitivity to different ocean tide models**

484

485 For the M2 constituent and height component, the three OTL softwares considered have been  
486 shown to output displacements with vector differences invariably no greater than 1-2 mm for  
487 sites adjacent to complicated coastlines and shallow seas (provided MRD is not used in  
488 OLFG/OLMPP), and often better than 0.2-0.5 mm when more than ~100 km inland or close to  
489 straighter coastlines and the deep oceans. This can therefore be considered the noise level of the  
490 convolution procedure. The horizontal displacement vector differences were considerably less.  
491 In this section an indication is provided of the magnitude of the commonly assumed biggest  
492 component of the OTL displacement error budget, namely ocean tide model quality.

493

494 M2 OTL height displacements were computed for the 387 IGS sites considered in section 3  
495 using the CARGA software and inputting each of the six modern ocean tide models CSR4.0,  
496 FES99, FES2004, GOT00.2, NAO.99b and TPXO.6.2. The CSR4.0 model used here is a  
497 filtered version – CSR4.0 grid cells over land were eliminated using the grid of the GOT00.2  
498 model. Vector differences between each model value and the six model mean value were  
499 computed and the RMS of these differences (i.e. inter-model agreement) used to assess model  
500 quality, which are plotted in Fig. 7. It can be seen that for a great many sites, particularly those  
501 inland, the OTL displacement is insensitive (<0.4 mm) to the choice of model, although  
502 discrepancies of nearly 3 mm arise for some coastal sites. Table 5 details the sites for which a  
503 discrepancy of greater than 1 mm arises, including the M2 amplitudes and Greenwich phase lags  
504 computed per model. It can be seen from Table 5 that for some sites such as TNML it is just  
505 one particular model (FES99) causing the inter-model discrepancy, although the discrepant  
506 model differs depending on global location. For example at PARC the discrepant model is  
507 NAO.99b, at TOW2 it is GOT00.2 and at AUCK it is FES2004. At some sites such as ALBH,

508 BAIE and NTUS, no one model is discrepant and the large RMS agreement is simply due to a  
509 larger scatter of the amplitude and phase values across all the models.

510

511 It is clear from Fig. 7 and Table 5 that OTL displacement values are sensitive to the choice of  
512 ocean tide model at the several millimetre level at some coastal sites. Furthermore, Penna et al.  
513 (2007) showed that RMS agreements between M2 height amplitudes computed using the  
514 SPOTL software with the CSR4.0, FES99, GOT00.2, NAO.99b and TPXO.6.1 models input can  
515 be as high as 8 mm in some regions such as the Weddell and Ross Seas, where there are no IGS  
516 sites. Which model is discrepant is location dependent, suggesting that it is not necessarily  
517 appropriate to use just a single model in global analyses, as was also suggested by Baker and  
518 Bos (2003). However, the IERS 2003 conventions do not stipulate any regional dependency in  
519 their recommendation to use either FES99 or GOT00.2. Meanwhile, the working version of  
520 updates (unratified) to these conventions available at  
521 <http://tai.bipm.org/iers/convupdt/convupdt.html> has changed the recommended model for global  
522 use to either FES2004 or TPXO.6.2, whilst recognising that other models might be preferred for  
523 internal consistency.

524

## 525 **8 Discussion and conclusions**

526

527 It has been clearly demonstrated that M2 OTL displacements (especially the height component)  
528 are sensitive to the refinement method adopted when the near ocean tide model grid cells do not  
529 perfectly fit the coast. If the local water mass redistribution approach of Scherneck (1991) is  
530 implemented and if the site is adjacent to complicated coastlines and shallow seas, errors of  
531 around 8 mm or 20% can arise for the height component, depending on the ocean tide model  
532 used. Particularly large errors have been shown to arise if the FES99 (0.25° resolution) or  
533 NAO.99b (0.5° resolution) models are used, attributed to their grids consistently overlapping the  
534 coastline which means that when MRD is applied, a large change in loading arises. Meanwhile,  
535 4-5 mm errors arise using the 0.5° resolution GOT00.2 model, which are less than when using  
536 NAO.99b despite the models' equivalent grid spacing. Thus the effect of MRD is dependent not  
537 just on the model's grid resolution, but on how much the grid overlaps the coastline. On  
538 average the GOT00.2 grid cells overlap the land as much as they leave a gap between the grid  
539 and the land, whereas the NAO.99b and FES99 grid cells overlap the land too much, resulting in  
540 loading errors when applying MRD. These errors have been confirmed using GPS  
541 measurements, since substantial energy remains at the M2 period in the GPS height time series  
542 amplitude spectra when using MRD, yet the energy reduces to the noise level when using  
543 CARGA (whose displacement values agree very closely with the OLFG/OLMPP NoMRD and  
544 SPOTL values). However, the grid of FES2004 has on average as many grid cells overlapping  
545 the coast as cells leaving a gap to the coast. This causes the MRD effect to be small for the  
546 FES2004 model.

547

548 Provided the MRD option is not used by the OLFG/OLMPP software package, this package,  
549 SPOTL and CARGA all compute M2 OTL height displacements that invariably agree at better

550 than the 1-2 mm level at coastal sites adjacent to complicated coastlines and shallow seas, and  
551 invariably better than 0.2 mm for sites more than ~100 km inland for all four models considered.  
552 When more than ~150 km inland, the OLFG/OLMPP MRD and NoMRD values are identical  
553 because no local refinement is applied at all. Expressing the inland differences as a proportion  
554 of the loading amplitude translates to ~2-5% (often less), which is in agreement with the  
555 comparisons of Agnew (1997) and Bos and Baker (2005), but contradicts the statement of Boy  
556 et al. (2003) that convolution errors of 10% can arise at Strasbourg (lon. 7.6838, lat. 48.6218) in  
557 north-east France. In order to model OTL displacement to an accuracy of around 1 mm, the  
558 three packages OLFG/OLMPP, SPOTL and CARGA can be considered practically  
559 interchangeable. The different model refinement methods for coastal cells when computing the  
560 OTL produce equivalent outputs, and suggest that for a displacement accuracy level of about 1  
561 mm, it does not matter if bilinear interpolation or the nearest grid cell value is used to determine  
562 the tidal amplitude at distances of more than  $10^\circ$  from the site. For the 387 IGS sites tested, the  
563 sensitivity of the horizontal displacements to the refinement method used was less than for the  
564 height component.

565  
566 Aside from model refinement at the coast and interpolation of model grid cells in the open  
567 ocean, contributions to the small differences between the OLFG/OLMPP, SPOTL and CARGA  
568 displacements arise from the choice of Green's function and the value for the density of sea  
569 water. To assess the effect of the Green's function used, the FES99 CARGA height values for  
570 the 387 IGS sites were recomputed using the Green's function of a Gutenberg-Bullen A Earth  
571 model (Farrell 1972), in addition to the default PREM Green's function of Francis and Mazzega  
572 (1990) which is used throughout the paper. For coastal sites, this changed the displacements by  
573 ~0.25 mm, although by about 0.8 mm at RIO2, whilst the change at inland sites was very small  
574 (< ~0.1 mm). Regarding the effect of sea water density, the average water density value for a

575 column of water can change by 1%. For sites with very large OTL displacement values of 20 to  
576 30 mm this corresponds to an error of 0.2-0.3 mm.

577

578 Whilst convolution errors have been shown, in general, to be not more than 1-2 mm, errors in  
579 the available ocean tide models remain a bigger contributor to errors in OTL displacement  
580 values. Height errors of up to around 3 mm RMS between the different modern models arise at  
581 IGS sites and up to around 8 mm in areas such as the Weddell Sea and Ross Ice Shelf where  
582 there are no IGS sites. No one model can yet be considered to best represent the tides in all  
583 regions of the world, with further research required to evaluate which model is most appropriate  
584 in different parts of the world. The models themselves still need some improvement. Notably  
585 some of the current global models lack any information on certain seas (e.g. NAO.99b omits the  
586 Ross Sea, TPXO.6.2 omits the Black Sea), which will cause problems for nearby sites. A  
587 possible solution is to develop regional tide models for these uncovered regions which is the  
588 approach adopted by SPOTL.

589

590 The widely used OTL web provider recommended in the IERS 2003 conventions (and suggested  
591 in the unratified updates) is driven by the OLF/OLMPP software. MRD was implemented for  
592 near coastal cells from 2001 until August 2007, when the option was switched off for the  
593 reasons outlined in this paper **and bilinear interpolation only is now used**. Therefore, for any  
594 GPS, DORIS, SLR or VLBI analyses that have applied OTL web provider generated  
595 displacement corrections computed during this window for sites within ~150 km of the coast,  
596 biased parameters will result. The size of such biases will depend on the distance of the site  
597 from the coast, the resolution of the model used, the shape of the nearby coastline, how much  
598 land overlap arises for the model's grid cells, and whether the site is adjacent to shallow seas or  
599 the deep oceans.

600

601 In this study, the OTL values represented displacements at the Earth's surface relative to the  
602 centre of mass of the undeformed solid Earth without atmosphere and oceans. In the ocean  
603 loading problem the distance between the solid Earth centre and the joint centre of mass of the  
604 Earth system (i.e. solid Earth and oceans) undergo tidal translations that are generated by  
605 hemispherical ocean mass exchange. In sensitive orbit calculations, this offset should be taken  
606 into account. From the perspective of a user of orbital products, for example those provided by  
607 the IGS in the case of GPS, it appears more practical if the translations are removed from the  
608 orbital products disseminated by the analysis centres. Many applications, such as relative GPS  
609 and VLBI, are insensitive to such translations anyway, and there is not yet clear evidence that  
610 the translation parameters are crucial and that they can be verified by orbit analyses. Since these  
611 parameters are somewhat uncertain in ocean tide modelling and also difficult to determine in  
612 altimetry, most space geodetic analysis centres do not apply them at present. Thus the  
613 assumption of the solid earth centre as a reference is consistent with the JPL fiducial orbit  
614 products used in this study. Any error would have to be tracked to second-order dynamic effects  
615 of the neglected offset to the joint mass centre. (Sensitive tests of orbit anomalies due to ocean  
616 tide mass induced frame centre translation are encouraged).

617

618 A centre of figure frame, as discussed in Blewitt (2003), did not need to be considered here – the  
619 centre of figure frame concept relates to unknown deformations and fits an undefining surface  
620 to the station positions. Included in the modelling of ocean loading are degree-one load Love  
621 numbers, which can be decomposed into a translation and a deformation part. However, this  
622 translation arises in the Earth's interior and does not displace the solid Earth's mass centre.  
623 From observations at the Earth's surface, this particular translation component cannot be  
624 distinguished from additional translations involving the mass centre.

625

626 This study only considered the (usually dominant) M2 constituent. Moreover, only a sample of  
627 globally distributed sites (the IGS network) was considered, along with a single more detailed  
628 test region (north-west Europe) that encompassed complicated coastlines and shallow seas, for  
629 which the (dominant) height component was considered only. High resolution intercomparisons  
630 of OTL softwares and ocean tide models should be undertaken for other coastal regions for  
631 height and horizontal displacements and various tidal constituents.

632

633

634 **Acknowledgments** The providers of the CSR4.0, FES99, FES2004, GOT00.2, NAO.99b and  
635 TPXO.6.2 ocean tide models are gratefully acknowledged, together with Duncan Agnew for  
636 making the SPOTL software freely available to the public. The UK NERC BIGF facility  
637 (<http://www.bigf.ac.uk>) is thanked for GPS data provision, and JPL for the GIPSY software and  
638 orbital products. Thanks to Matt King for his initial development of the GPS data processing  
639 method. Many of the figures were produced using the GMT v4.2 software (Wessel and Smith  
640 1998). Penna was funded by UK NERC grant NE/C003438/1 and Bos by Fundação para a  
641 Ciência e a Tecnologia (FCT), through grant SFRH/BPD/26985/2006. Constructive reviews by  
642 Duncan Agnew and Jean-Paul Boy are acknowledged.

643

644

645 **References**

646

647 Agnew DC (1997) NLOADF: A program for computing ocean-tide loading. *J Geophys Res*  
648 102(B3):5109-5110

649 Allinson CR, Clarke PJ, Edwards SJ, King MA, Baker TF, Cruddace PR (2004) Stability of  
650 direct GPS estimates of ocean tide loading. *Geophys Res Lett* 31(15). DOI  
651 10.1029/2004GL020588

652 Baker TF, Bos MS (2003) Validating Earth and ocean tide models using tidal gravity  
653 measurements. *Geophys J Int* 152(2):468-485

654 Blewitt G (2003) Self-consistency in reference frames, geocenter definition, and surface loading  
655 of the solid Earth. *J Geophys Res* 108(B2): 2103. DOI:10.1029/2002JB002082

656 Bos MS, Baker TF (2005) An estimate of the errors in gravity ocean tide loading computations.  
657 *J Geod* 79(1-3):50-63

658 Bos MS, Baker TF, Røthing K, Plag H-P (2002) Testing ocean tide models in the Nordic seas  
659 with tidal gravity observations. *Geophys J Int* 150(3):687-694

660 Boy J-P, Llubes M, Hinderer J, Florsch N (2003) A comparison of tidal ocean loading models  
661 using superconducting gravimeter data. *J Geophys Res* 108(B4):2193. DOI  
662 10.1029/2002JB002050

663 Dow JM, Neilan RE, Gendt G (2005) The International GPS Service: Celebrating the 10th  
664 anniversary and looking to the next decade. *Advances in Space Research* 36:320-326

665 Eanes RJ, Bettadpur S (1996) The CSR3.0 Global Ocean Tide Model: Diurnal and Semi-  
666 Diurnal Ocean Tides from TOPEX/POSEIDON Altimetry. CSR-TM-96-05 The University  
667 of Texas Center for Space Research.

668 Egbert GD, Bennett AF, Foreman MGG (1994) TOPEX/POSEIDON tides estimated using a  
669 global inverse model. *J Geophys Res* 99(C12):24,821-24852

670 Egbert GD, Erofeeva SY (2002) Efficient inverse modeling of barotropic ocean tides. *J Atm*  
671 *Oceano Tech* 19(2):183-204

672 Farrell WE (1972) Deformation of the Earth by surface loads. *Rev Geophys Space Phys*  
673 10(3):761-797

674 Francis O, Mazzega P (1990) Global charts of ocean tide loading effects. *J Geophys Res*  
675 95(C7):11411–11424

676 Hendershott MC and Munk W (1970) Tides. *Ann Rev Fluid Mech* 2:205-224

677 King M (2006) Kinematic and static GPS techniques for estimating tidal displacements with  
678 application to Antarctica. *J Geodyn* 41(1-3):77-86

679 King MA, Penna NT, Clarke PJ, King EC (2005) Validation of ocean tide models around  
680 Antarctica using onshore GPS and gravity data. *J Geophys Res* 110(B8): B08401. DOI  
681 10.1029/2004JB003390

682 King MA, Watson CW, Penna NT, Clarke PJ (2008) Subdaily signals in GPS observations and  
683 their effect at semiannual and annual periods. *Geophys Res Lett* 35: L03302.  
684 DOI:10.1029/2007GL032252.

685 Le Provost C, Genco ML, Lyard F, Vincent P, Canceil P (1994) Spectroscopy of the world  
686 ocean tides from a finite-element hydrodynamic model. *J Geophys Res* 99(C12):24777-  
687 24797

688 Lefèvre F, Lyard FH, Le Provost C, Schrama EJO (2002) FES99: A global tide finite element  
689 solutions assimilating tide gauge and altimetric information. *J Atmos Ocean Technol*,  
690 19(9):1345-1356

691 Longman IM (1962) A Green's function for determining the deformation of the Earth under  
692 surface mass loads, 1. Theory. *J Geophys Res* 67(2):845-850

693 Longman IM (1963) A Green's function for determining the deformation of the Earth under  
694 surface mass loads, 2. Computation and Numerical Results. *J Geophys Res* 68(2):485-496

695 Lyard F, Lefèvre F, Letellier T, Francis O (2006) Modelling the global ocean tides: Modern  
696 insights from FES2004. *Ocean Dynam* 56(5-6):394-415

697 Matsumoto K, Takanezawa T, Ooe M (2000) Ocean tide models developed by assimilating  
698 TOPEX/POSEIDON altimeter data into hydrodynamical model: A global model and a  
699 regional model around Japan. *J. Oceanogr* 56:567-581

700 Matsumoto K, Sato T, Takanezawa T, Ooe M (2001) GOTIC2: A program for computation of  
701 oceanic tidal loading effect. *J Geod Soc Japan* 47:243-248

702 McCarthy DD, Petit G (2004) IERS Conventions 2003. IERS Technical Note 32.

703 Melachroinos SA, Biancale R, Llubes M, Perosanz F, Lyard F, Vergnolle M, Bouin M-N,  
704 Masson F, Nicolas J, Morel L, Durand S (2007) Ocean tide loading (OTL) displacements  
705 from global and local grids: comparisons to GPS estimates over the shelf of Brittany, France.  
706 *J Geod* DOI 10.1007/s00190-007-0185-6

707 Penna NT, King MA, Stewart MP (2007) GPS height time series: Short-period origins of  
708 spurious long-period signals. *J Geophys Res* 112(B02402). DOI 10.1029/2005JB004047

709 Petrov L, Ma CP (2003) Study of harmonic site position variations determined by very long  
710 baseline interferometry. *J Geophys Res* 108(B4): 2190. DOI 10.1029/2002JB001801

711 Press WH, Teukolsky SA, Vetterling WT, Flannery BP (1992) *Numerical recipes in Fortran 77:*  
712 *the art of scientific computing*. 2<sup>nd</sup> edition Cambridge University Press

713 Ray RD (1999) A global ocean tide model from TOPEX/POSEIDON altimetry: GOT99.2.  
714 NASA Tech Memo TM-209478 58 pp

715 Scargle JD (1982) Studies in astronomical time series analysis. II. Statistical aspects of spectral  
716 analysis of unevenly spaced data. *Astrophysical Journal* 263:835-853

717 Scherneck H-G (1991) A parametrized solid earth tide model and ocean tide loading effects for  
718 global geodetic base-line measurements. *Geophys J Int* 106(3):677-694

719 Scherneck H-G (1993) Ocean tide loading: Propagation of errors from the ocean tide into  
720 loading coefficients. *Manuscripta Geodaetica* 18:677-694

721 Schwiderski EW (1980) On charting global ocean tides. *Rev Geophys Space Phys* 18(1):243-  
722 268

723 Shum CK, Woodworth PL, Andersen OB, Egbert GD, Francis O, King C, Klosko SM, Le  
724 Provost C, Li X, Molines JM, Parke ME, Ray RD, Schlax ML, Stammer D, Tierney CC,  
725 Vincent P, Wunch CI (1997) Accuracy assessment of recent ocean tide models. *J Geophys*  
726 *Res* 102(C11):25173-25194

727 Thomas ID, King MA, Clarke PJ (2007) A comparison of GPS, VLBI and model ocean tide  
728 loading displacements. *J Geod* 81:359-368. DOI 10.1007/s00190-006-0118-9

729 Urschl C, Dach R, Hugentobler U, Schaer S, Beutler G (2005) Validating ocean tide loading  
730 models using GPS. *J Geod* 78:616-625

731 Wessel P, Smith WHF (1998) New, improved versions of the Generic Mapping Tools released.  
732 *Eos Trans AGU* 79(47): 579

733

734 **FIGURE CAPTIONS**

735

736 **Fig. 1** M2 OTL height displacement vector differences between the OLFG/OLMPP, SPOTL  
737 and CARGA softwares for 387 IGS sites when using the FES99 and FES2004 ocean tide  
738 models

739

740 **Fig. 2** M2 OTL height displacement amplitudes and Greenwich phase lags for a 0.125° grid  
741 across north-west Europe, computed using CARGA with the FES2004 ocean tide model

742

743 **Fig. 3** OLFG/OLMPP (MRD) minus CARGA M2 OTL height displacement vector differences  
744 for a 0.125° grid across north-west Europe when using the GOT00.2, FES99, NAO.99b and  
745 FES2004 ocean tide models

746

747 **Fig. 4** SPOTL minus CARGA M2 OTL height displacement vector differences for a 0.125° grid  
748 across north-west Europe when using the GOT00.2, FES99, NAO.99b and FES2004 ocean tide  
749 models

750

751 **Fig. 5** OLFG/OLMPP (NoMRD) minus CARGA M2 OTL height displacement vector  
752 differences for a 0.125° grid across north-west Europe when using the GOT00.2, FES99,  
753 NAO.99b and FES2004 ocean tide models

754

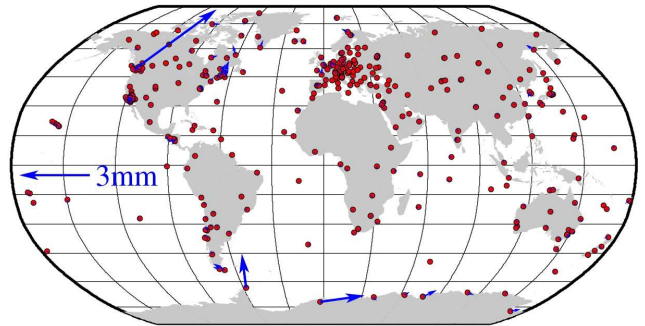
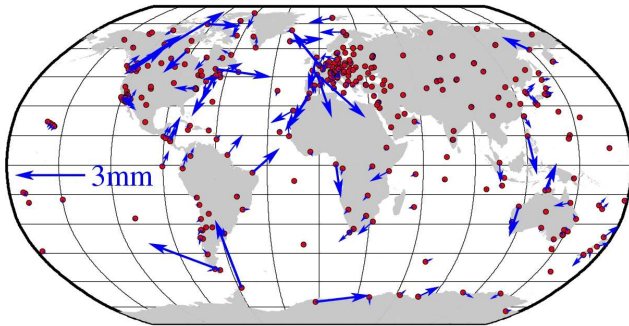
755 **Fig. 6** GPS height amplitude spectra for OLFG/OLMPP (MRD) and CARGA solutions for  
756 ocean tide models FES99 at site APPL, GOT00.2 at GLAS, NAO.99b at MALG, and FES2004  
757 at NEWC

758

759 **Fig. 7** RMS vector differences of M2 OTL height displacements for 387 IGS sites, computed  
760 using CARGA and the CSR4.0, FES99, FES2004, GOT00.2, NAO.99b and TPXO.6.2 ocean  
761 tide models  
762  
763

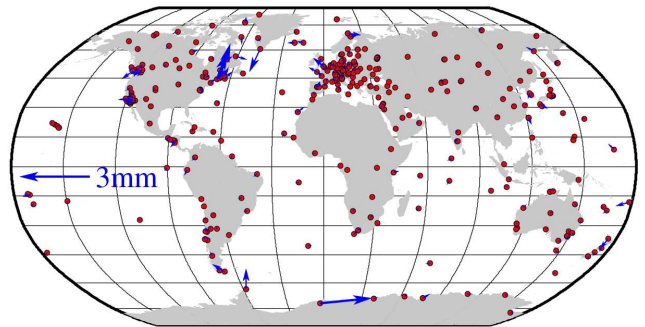
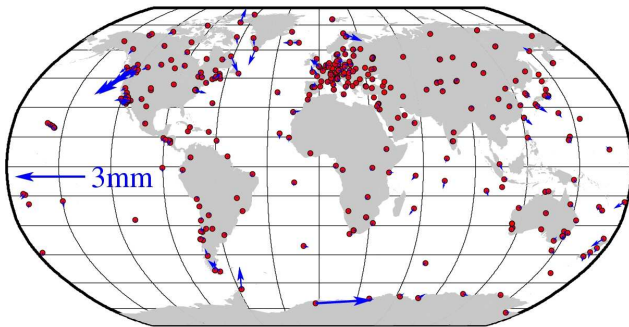
FES99 OLFG/OLMPP (MRD) - CARGA

FES2004 OLFG/OLMPP (MRD) - CARGA



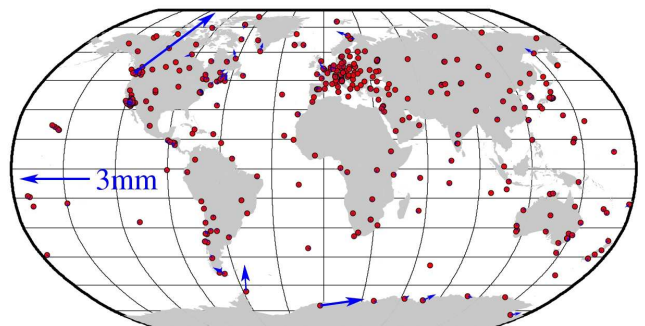
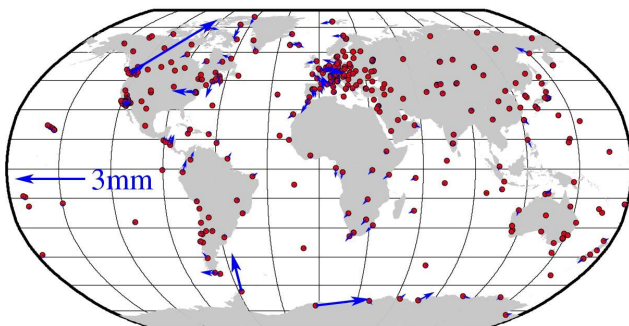
FES99 SPOTL - CARGA

FES2004 SPOTL - CARGA



FES99 OLFG/OLMPP (NoMRD) - CARGA

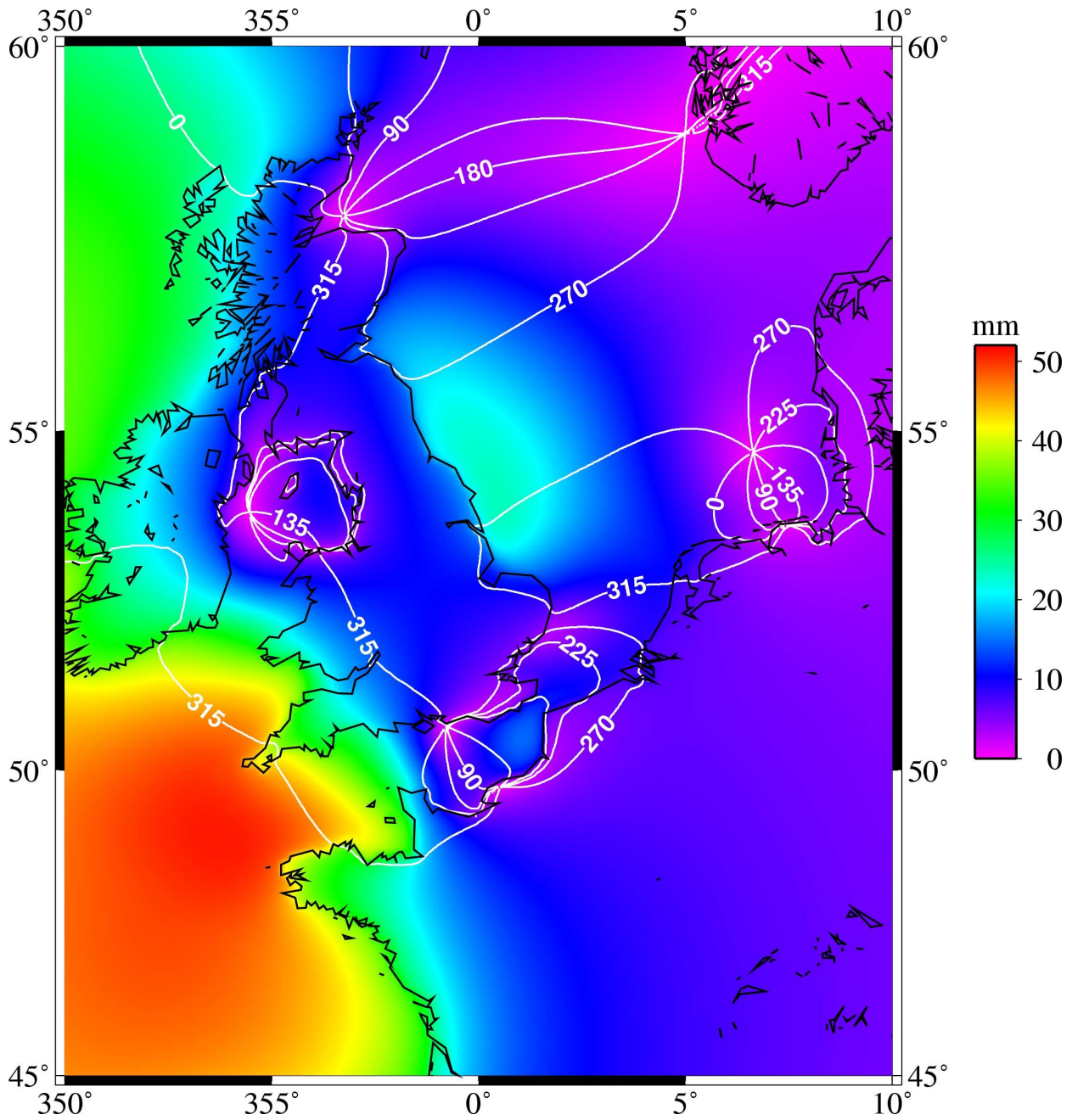
FES2004 OLFG/OLMPP (NoMRD) - CARGA



765  
766  
767  
768

769 **Fig. 1** M2 OTL height displacement vector differences between the OLFG/OLMPP, SPOTL  
770 and CARGA softwares for 387 IGS sites when using the FES99 and FES2004 ocean tide  
771 models

772



773

774

775

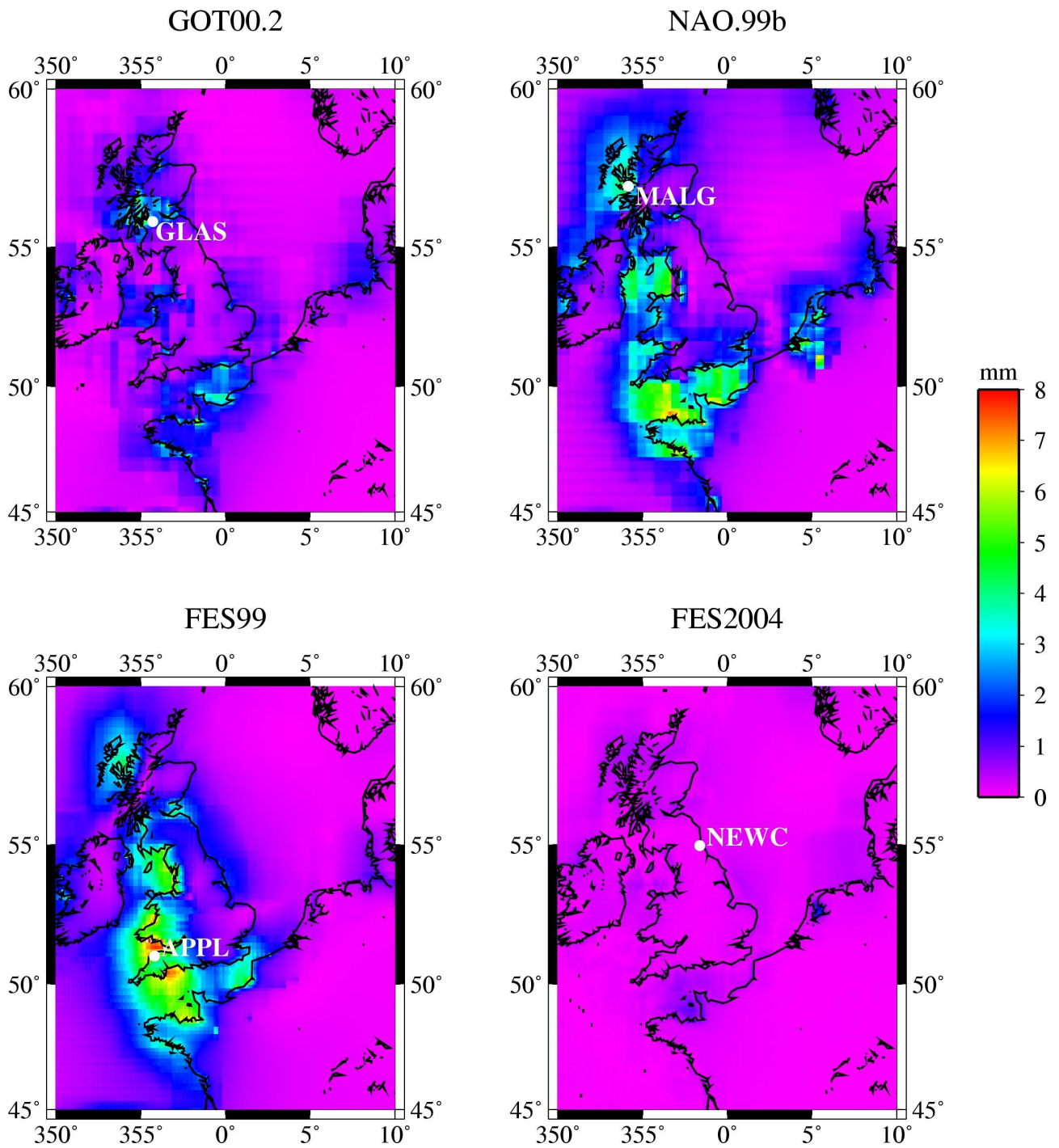
776

777

**Fig. 2** M2 OTL height displacement amplitudes and Greenwich phase lags for a 0.125° grid

778 across north-west Europe, computed using CARGA with the FES2004 ocean tide model

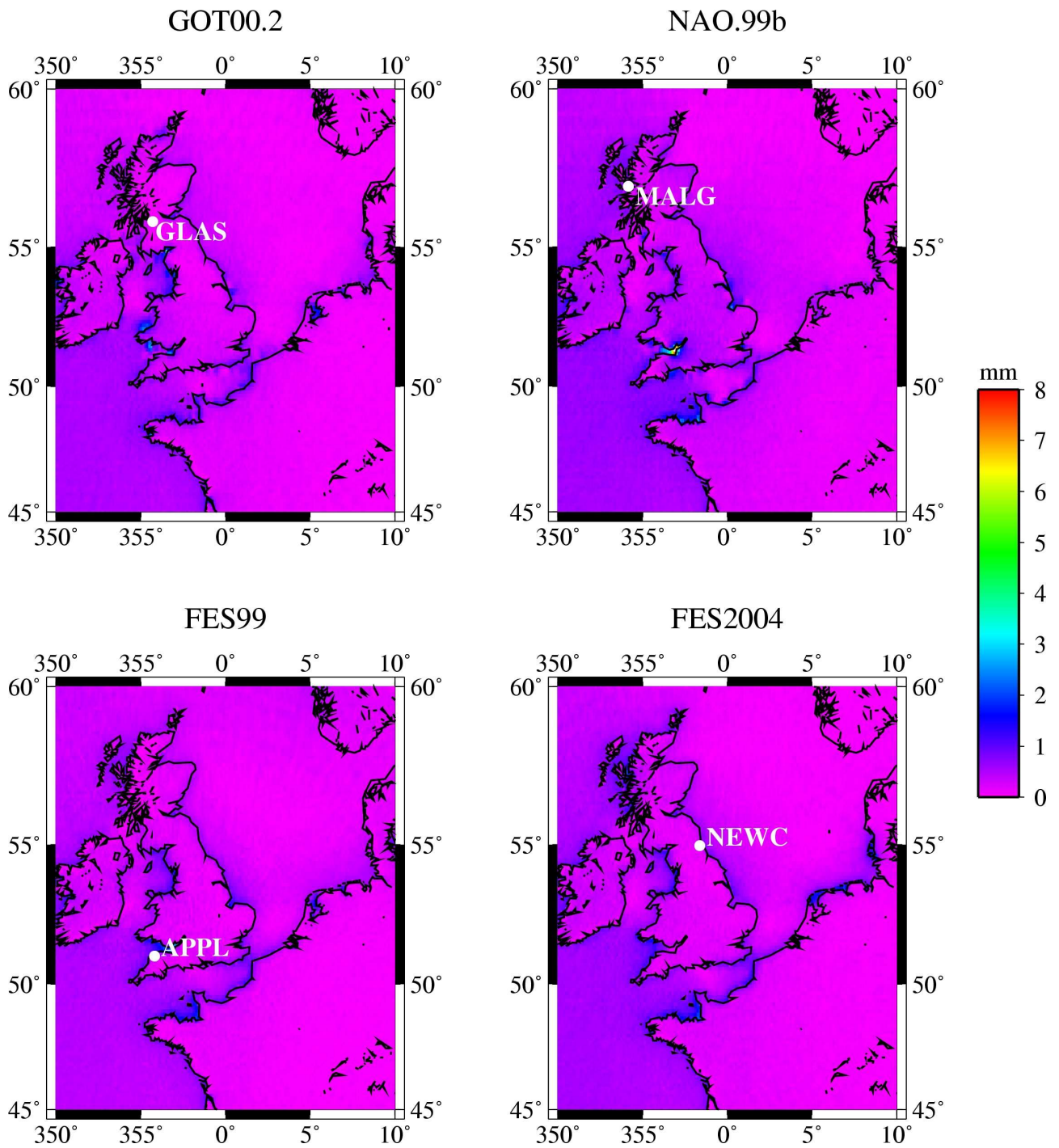
779



781  
782  
783  
784

785 **Fig. 3** OLFG/OLMPP (MRD) minus CARGA M2 OTL height displacement vector differences  
786 for a 0.125° grid across north-west Europe when using the GOT00.2, FES99, NAO.99b and  
787 FES2004 ocean tide models

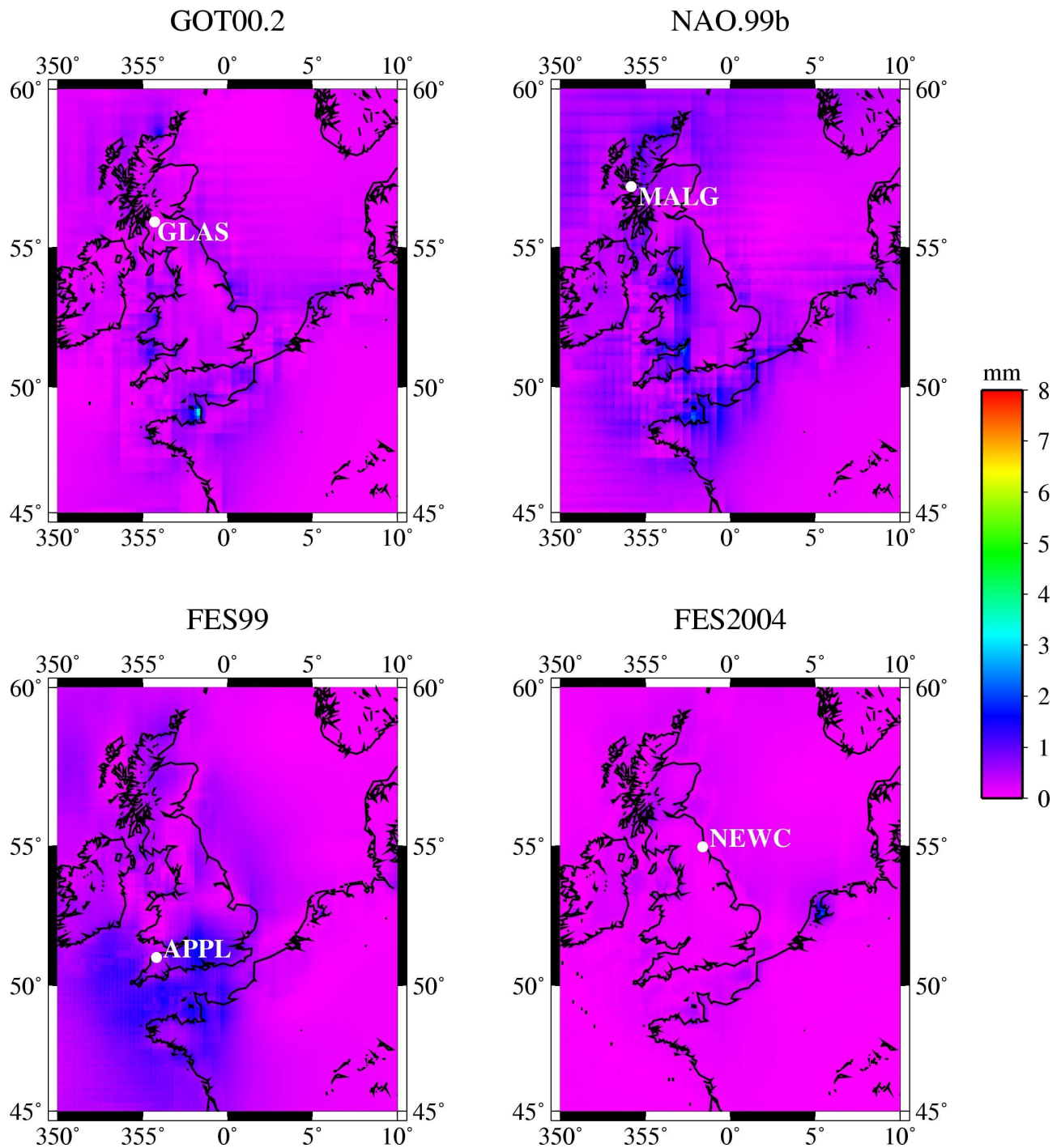
788



790  
791  
792  
793

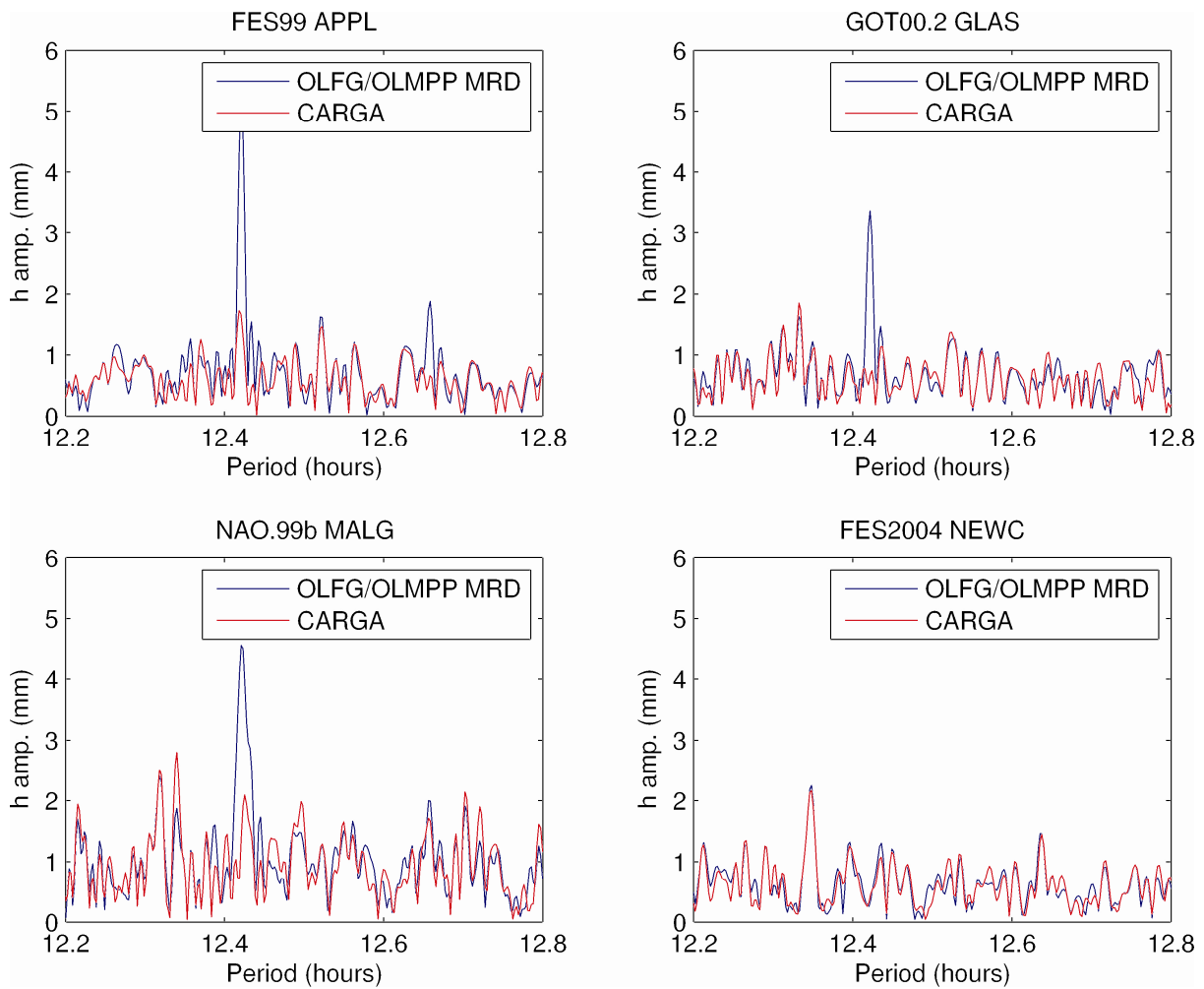
794 **Fig. 4** SPOTL minus CARGA M2 OTL height displacement vector differences for a 0.125° grid  
795 across north-west Europe when using the GOT00.2, FES99, NAO.99b and FES2004 ocean tide  
796 models

797



799  
 800  
 801  
 802  
 803  
 804  
 805  
 806

**Fig. 5** OLFG/OLMPP (NoMRD) minus CARGA M2 OTL height displacement vector differences for a  $0.125^\circ$  grid across north-west Europe when using the GOT00.2, FES99, NAO.99b and FES2004 ocean tide models



808

809

810

811

812

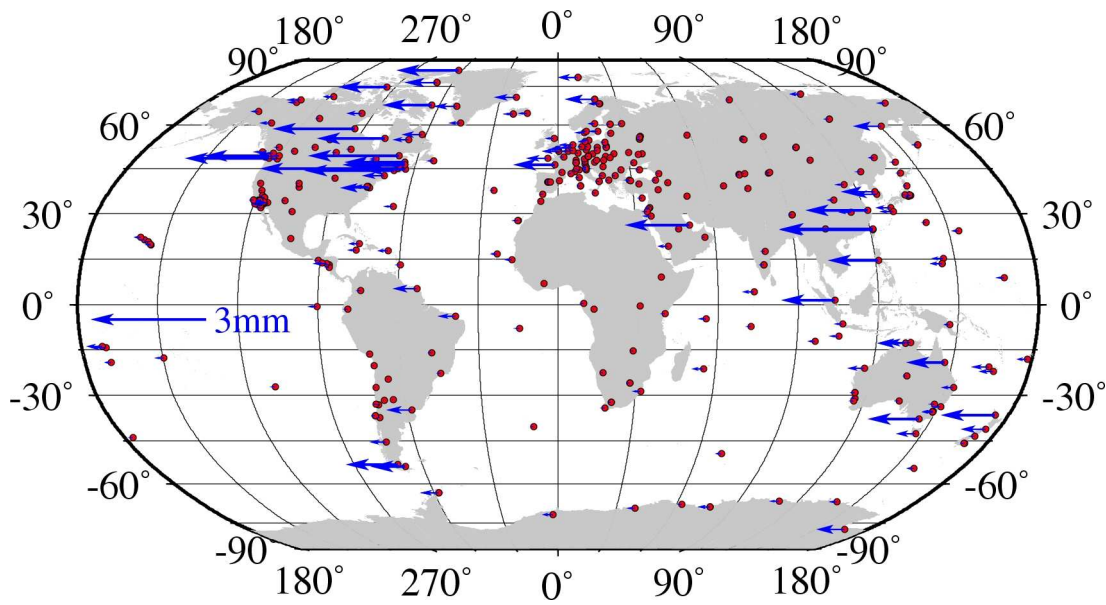
813

814

815

**Fig. 6** GPS height amplitude spectra for OLFG/OLMPP (MRD) and CARGA solutions for ocean tide models FES99 at site APPL, GOT00.2 at GLAS, NAO.99b at MALG, and FES2004 at NEWC

816



817  
818  
819  
820

821 **Fig. 7** RMS vector differences of M2 OTL height displacements for 387 IGS sites, computed  
822 using CARGA and the CSR4.0, FES99, FES2004, GOT00.2, NAO.99b and TPXO.6.2 ocean  
823 tide models

824  
825

826

827 **Table 1** Tally of M2 OTL height displacement vector differences between the different  
 828 softwares for 387 IGS sites when using the FES99 and FES2004 models  
 829

Vector difference magnitude	OLFG/OLMPP (MRD) – CARGA	FES99			FES2004	
		SPOTL – CARGA	OLFG/OLMPP (No MRD) – CARGA	OLFG/OLMPP (MRD) – CARGA	SPOTL – CARGA	OLFG/OLMPP (No MRD) – CARGA
< 0.2 mm	199	298	286	350	318	358
< 0.5 mm	305	369	364	378	373	381
> 1.0 mm	34	5	5	4	6	3

830

831

832

833

834 **Table 2** Tally of M2 OTL east displacement vector differences between the different softwares  
 835 for 387 IGS sites when using the FES99 and FES2004 models  
 836

Vector difference magnitude	OLFG/OLMPP (MRD) – CARGA	FES99			FES2004	
		SPOTL – CARGA	OLFG/OLMPP (No MRD) – CARGA	OLFG/OLMPP (MRD) – CARGA	SPOTL – CARGA	OLFG/OLMPP (No MRD) – CARGA
< 0.2 mm	366	383	374	383	383	383
< 0.5 mm	383	387	385	387	387	387
> 1.0 mm	----	----	----	----	----	----

837

838

839

840

841 **Table 3** Tally of M2 OTL north displacement vector differences between the different  
 842 softwares for 387 IGS sites when using the FES99 and FES2004 models  
 843

Vector difference magnitude	OLFG/OLMPP (MRD) – CARGA	FES99			FES2004	
		SPOTL – CARGA	OLFG/OLMPP (No MRD) – CARGA	OLFG/OLMPP (MRD) – CARGA	SPOTL – CARGA	OLFG/OLMPP (No MRD) – CARGA
< 0.2 mm	355	383	371	383	384	383
< 0.5 mm	384	384	385	385	384	385
> 1.0 mm	----	----	----	----	----	----

844

845

846

847

848 **Table 4** North-west Europe site details and M2 OTL height displacement amplitudes (A) and  
 849 Greenwich phase lags ( $\Phi$ ) for different softwares. Latitudes and longitudes are positive in the  
 850 north and east directions respectively.  
 851

Site	Lon. (°)	Lat. (°)	Model	OLFG/OLMPP (MRD)		CARGA		SPOTL		OLFG/OLMPP (NoMRD)	
				A (mm)	$\Phi$ (°)	A (mm)	$\Phi$ (°)	A (mm)	$\Phi$ (°)	A (mm)	$\Phi$ (°)
APPL	355.8003	51.0569	FES99	38.20	327.5	32.21	322.5	32.16	322.5	32.77	323.0
GLAS	355.7035	55.8540	GOT00.2	12.39	312.1	9.76	309.2	9.69	309.4	9.67	309.4
MALG	354.1716	57.0061	NAO.99b	23.96	341.8	19.94	337.9	19.40	337.9	19.77	338.8
NEWC	358.3834	54.9791	FES2004	13.88	287.0	13.80	287.0	13.97	286.4	13.92	286.7

852

853

854 **Table 5** Predicted M2 OTL height displacement amplitudes (A) and Greenwich phase lags ( $\Phi$ )  
 855 from six ocean tide models using the CARGA software for IGS sites for which the RMS of the  
 856 vector differences (mm) from the six model mean was greater than 1 mm. Latitudes and  
 857 longitudes are positive in the north and east directions respectively.  
 858

Site	Lon (°)	Lat (°)	CSR4.0		FES99		FES2004		GOT00.2		NAO.99b		TPXO.6.2		Vector RMS Diffn.
			A (mm)	$\Phi$ (°)											
ALBH	236.5126	48.3898	17.0	72	20.8	68	16.1	78	17.0	72	15.5	73	19.8	69	2.2
ALRT	297.6596	82.4943	0.6	111	0.9	261	0.9	220	0.4	111	3.7	88	1.0	236	1.6
AUCK	174.8344	-36.6028	27.7	56	27.9	55	24.9	59	27.5	56	27.4	59	27.7	54	1.4
BAHR	50.6081	26.2091	5.2	253	3.4	296	6.6	259	6.1	256	7.1	257	6.2	258	1.7
BAIE	291.7367	49.1868	5.9	146	2.9	106	4.4	84	5.7	148	4.0	84	3.9	94	2.4
BARH	291.7783	44.3950	9.5	211	13.4	227	13.4	236	13.9	235	13.8	235	12.4	231	2.3
CHUR	265.9113	58.7591	6.4	198	5.6	182	10.8	181	9.4	182	10.3	187	9.1	177	2.1
EPRT	293.0079	44.9087	9.5	205	13.8	222	16.0	242	16.3	238	15.9	234	13.3	229	3.6
ESCU	295.2013	47.0734	6.3	154	6.7	116	5.9	154	6.6	157	6.3	142	6.2	145	1.6
HLFX	296.3887	44.6835	13.7	169	13.5	169	13.2	180	14.0	176	12.7	180	13.5	1701	1.2
KUUJ	282.2546	55.2784	7.3	168	4.9	165	9.9	158	9.1	157	8.7	157	8.3	153	1.8
LROC	358.7807	46.1589	27.5	281	28.2	282	27.6	287	27.8	282	27.2	282	27.5	281	1.1
MOBS	144.9753	-37.8294	6.8	172	3.7	153	6.2	164	7.1	170	7.1	172	6.5	172	1.3
NANO	235.9135	49.2948	18.4	72	17.5	74	15.8	76	18.4	73	15.9	75	20.4	71	1.7
NTUS	103.6799	1.3458	5.1	196	4.9	180	6.1	184	5.6	186	4.3	197	5.3	153	1.4
PARC	289.1201	-53.1370	5.9	143	6.1	152	5.8	150	5.6	144	6.8	127	5.4	118	1.4
PIMO	121.0777	14.6357	8.1	139	6.7	145	9.9	134	9.1	136	10.3	134	9.5	135	1.3
QIKI	295.9663	67.5593	13.7	119	11.8	117	13.2	117	13.6	117	11.0	125	12.7	112	1.3
RESO	265.1067	74.6908	7.6	35	4.5	35	5.3	26	7.5	35	5.1	41	6.0	32	1.3
SHAO	121.2004	31.0996	7.0	193	4.1	212	6.7	202	8.4	210	7.8	211	7.8	199	1.6
SHE2	295.4480	46.2207	7.9	164	7.5	155	7.2	192	8.3	178	7.1	175	7.6	163	1.6
TCMS	120.9874	24.7980	10.2	209	7.4	235	12.2	209	11.8	208	12.0	207	11.7	201	2.4
TNML	120.9873	24.7980	10.2	209	7.4	235	12.2	209	11.8	208	12.0	207	11.7	201	2.4
TWTF	121.1645	24.9536	10.6	200	7.3	224	12.3	202	12.0	201	12.2	200	12.1	194	2.4
UNBJ	293.3583	45.9502	7.3	172	6.9	179	6.8	199	7.5	194	6.8	197	6.8	183	1.3

859

860

861